# Ultralow Loading Cobalt-Based Nanocatalyst for Benign and Efficient Aerobic Oxidation of Allylic Alcohols and Biobased Olefins

Xin Zhao,[†] Yan Zhou,[†] Kuan Huang,[‡] Changzhi Li,*,[§] and Duan-Jian Tao*,[†]

[†]College of Chemistry and Chemical Engineering, Jiangxi Normal University, Nanchang 330022, China

[‡]Key Laboratory of Poyang Lake Environment and Resource Utilization of Ministry of Education, School of Resources Environmental and Chemical Engineering, Nanchang University, Nanchang 330031, China

[§]State Key Laboratory of Catalysis, Dalian Institute of Chemical Physics, Chinese Academy of Sciences, Dalian 116023, China

S *Supporting Information*

ABSTRACT: The synthesis of α,β-unsaturated ketones from aerobic oxidation of allylic alcohols and biobased olefins serves as an important topic in green and sustainable chemistry. In this work, we report the utilization of a sacrificial template ZIF-8 for preparation of mesoporous $Co_{0.05}/N-C$ material with an ultralow cobalt loading of 0.05 wt %, in which the excellent catalytic performance in aerobic oxidation of α-pinene and cinnamyl alcohol was achieved with an 85% yield of verbenone and a yield of cinnamaldehyde, respectively. The results of control experiments and several characterization investigations further illustrate that the sacrificial template ZIF-8 plays a key role to disperse well metallic cobalt in the $Co_{0.05}/N-C-800$ catalyst and an appropriate cobalt content of 0.05 wt % is beneficial for benign and efficient aerobic oxidation of various allylic alcohols and biobased olefins. In addition, the $Co_{0.05}/N-C-800$ catalyst also exhibited good stability and reusability for recovering and reusing at least six times without obvious decrease in catalytic activity. The presented efficient nanocatalyst thus triggers facile synthesis of a series of α,β-unsaturated aldehydes/ketones in high yields.

KEYWORDS: Allylic oxidation, Co/N−C catalyst, Biobased olefin, α-Pinene, Cinnamyl alcohol
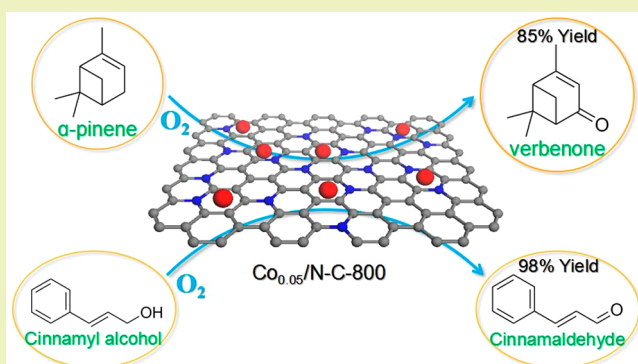
INTRODUCTION

The allylic oxidation of olefins to directly produce α,β-unsaturated ketones is one of the most important transformations in the research of C−H bond activation.[1−4] α-Pinene is a common renewable bio-olefin and has received much attention in recent years.[5−7] The oxidation of α-pinene yields valuable products such as α-pinene oxide, campholenic aldehyde, verbenol, and verbenone. These products are key building blocks in the fields of natural products, biopharmaceuticals, flavors, and fragrances.[8,9] As an important α,β-unsaturated ketone, verbenone can be employed for the preparation of menthol, taxol, and vitamins A and E.[10,11] Also, it can be used as repellent of *Dendroctonus valens* LeConte, making great contributions to the protection of the forestry ecological environment. Thus, benign and efficient production of verbenone via allylic oxidation of α-pinene is highly desirable.

In the past decades, great efforts have been made to improve catalytic efficiency in the production of verbenone. Metal salts, metal complexes, supported noble metals, and metal−organic frameworks (MOFs) have been employed as catalysts for this transformation.[12,13] For example, Mikkola et al. reported $AuCu/TiO_2$-catalyzed oxidation of α-pinene with a 46% yield

of verbenone using TBHP as the oxidant.[14] Kholdeeva and co-workers used Co-POM/MIL-101 as the catalyst for selective oxidation of α-pinene by molecular oxygen, resulting in 27% yield of verbenone.[15] Kleist et al. tried a Mn-containing MOF as the catalyst for aerobic oxidation of α-pinene; however, the yield of verbenone was less than 5%.[16] These findings show that the yield and selectivity of verbenone from the allylic oxidation of α-pinene is not entirely satisfied, and some catalytic systems even employ strong oxidants such as H_2O_2 and TBHP as the terminal oxidant. Hence, novel catalyst with high efficiency for benign oxidation of α-pinene to produce verbenone is still urgently to be developed in the green and sustainable chemistry.

Recently, atomically dispersed metal atom supported catalysts have been regarded as an effective method to maximize the atom utilization of metals for catalysis.[17−19] With ultralow metal loading, such exciting materials have shown excellent catalytic performance toward diverse reactions under mild condition, such as oxidation, hydrogenation, and

electrocatalysis.[20−23] Inspired by the isolated single iron atoms catalyst derived from ZIF-8,[24] it is promising and highly conceivable to confine and disperse other metal atoms with good dispersion and ultralow loading using ZIF-8 as the sacrificial template. The as-prepared materials thereby can be introduced into the selective oxidation of α-pinene, and they would show great potential for efficient and environmentally friendly production of verbenone.

Herein, we report the utilization of a sacrificial template ZIF-8 to prepare mesoporous Co/N−C materials with ultralow cobalt loadings (0.01~0.2 wt %), in which these Co/N−C materials shows excellent catalytic performance in aerobic oxidation of α-pinene to verbenone using ambient oxygen molecules as the benign oxidant. These highly efficient catalysts are designated as Co_x/N−C-y (x = Co loading in wt %; y = annealing temperature). The key to this preparation process is to prepare the Co(II)acetylacetonate@ZIF-8 composite. During thermal calcination, the ZIF-8 shell acts as structural template as well as N-doping and carbon source, and thus, the resulting Co_x/N−C-y materials could be obtained with very good dispersion and ultralow cobalt loading. The structures of these Co_x/N−C-y samples were characterized by inductively coupled plasma-atomic emission spectroscopy (ICP-AES), Raman spectroscopy, X-ray powder diffraction (XRD), transmission electron microscopy (TEM), high resolution transmission electron microscopy (HRTEM), and X-ray photoelectron spectroscopy (XPS). In addition, the oxidation reaction of other allylic alcohols and biobased olefins and the reusability of Co_x/N−C-y catalysts were also studied.

■ EXPERIMENTAL SECTION

Materials. α-Pinene (99%), 2-methylimidazole (99%), and cobalt(II) acetylacetonate ($Co(acac)_2$, 99%) were purchased from Shanghai Macklin Biochemical Co., Ltd. and used without further purification. All the other chemicals were used as received without further treatment.

Synthesis of Co_x/N−C-y Catalyst. Typically, 2-methylimidazole (60 mmol, 5 g) and $Zn(NO_3)_2·6H_2O$ (15 mmol, 4.5 g) were dissolved in 100 mL of methanol, respectively, and then the prepared solutions were added to a beaker. Subsequently, $Co(acac)_2$ (0.1 mmol, 0.026 g) was added into the mixture with vigorous stirring for 8 h at 25 °C. The mixture solutions were charged into a 100 mL stainless-steel autoclave and heated at 120 °C for 4 h. The obtained purple precipitation was separated by centrifugation and washed with DMF and methanol three times. The product (Co@ZIF-8) was then dried at 85 °C under vacuum for 24 h. The Co@ZIF-8 sample was loaded into a quartz boat in a tubular furnace and heated at 800 °C in Ar atmosphere for 2 h with a heating rate of 10 °C/min. The obtained black powder was cooled to room temperature and designated as $Co_{0.05}$/N−C-800. Accordingly, the sample $Co_{0.05}$/N−C-950 was heated at 950 °C in Ar atmosphere for 2 h with a heating rate of 10 °C/min. In addition, the preparation procedure of $Co_{0.01}$/N−C-800 and $Co_{0.20}$/N−C-800 catalysts was similar to that of $Co_{0.05}$/N−C-800, in which the precursor $Co(acac)_2$ was charged with dosages of 0.02 and 0.4 mmol, respectively.

Characterization of Co_x/N−C-y Catalyst. The mixture of HNO_3/HCl (1/3 ratio) was used to completely dissolve the Co_x/N−C-y sample, and then the Co loading in the Co_x/N−C-y samples were measured by ICP-AES (Agilent 720 instrument). The Brunauer−Emmett−Teller (BET) surface area, pore size distribution, and average pore diameter of the Co_x/N−C-y sample were characterized by nitrogen adsorption/desorption analysis (Quantachrome Quadrasorb SI Instrument) at −196 °C. The samples were degassed at 150 °C for 8 h before the measurements. XRD patterns of samples were obtained on a Rigaku RINT-2200 X-ray diffractometer, using a Cu Kα source at 40 kV and 20 mA. Raman spectra were

recorded on a LabRAM HR spectrometer with an argon laser (632 nm) as an excitation source. The morphology and sizes of the samples were studied by TEM and HRTEM (JEM-2100 from JEOL). The elemental composition of the sample surfaces was tested by XPS (Thermo Scientific ESCALAB 250Xi, Al Kα radiation source).

Catalytic Reaction. The selective oxidation of α-pinene to verbenone was carried out in a 10 mL round-bottomed flask containing α-pinene (1.0 g) and $Co_{0.05}$/N−C-800 catalyst (0.05 g). The reaction mixture was heated to 85 °C for 24 h with an oxygen balloon under constant stirring. The selective oxidation of cinnamyl alcohol was performed in a 25 mL round-bottom flask containing cinnamyl alcohol (1.0 mmol), $Co_{0.05}$/N−C-800 catalyst (0.05 g), and toluene (3 mL). The flask was vigorously stirred at 100 °C for 30 h under an oxygen balloon.

After the reaction, the catalyst was first separated from the reaction mixture by simple filtration. Then a quantity of internal standard acetonitrile (≥99.9%) was added to the mixture to quantify the products (Figure S1). The samples were identified by gas chromatography−mass spectrometry (GC-MS) (Thermo Trace 1300 GC-ISQ) and quantified by using a GC-FID (Agilent 7890B) equipped with a capillary column HP-5 (methyl polysiloxane, 30 m × 0.32 mm × 1 μm). The injector and detector temperatures were set as 280 and 250 °C, respectively. The column temperature was increased from 60 to 280 °C at 10 °C·min^{-1}, holding at 280 °C for 2 min.

■ RESULTS AND DISCUSSION

Characterization of Co_x/N−C-800 Catalyst. To study the structural feature of Co/N−C-800 samples, several
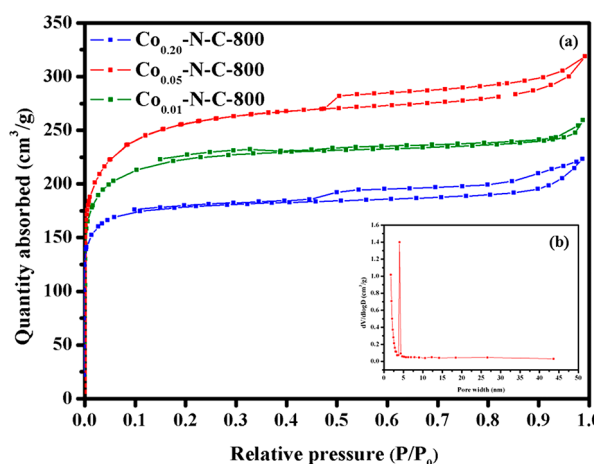

Figure 1. (a) N_2 adsorption−desorption isotherms of Co_x/N−C-800 at −196 °C and (b) BJH pore-size distributions of $Co_{0.05}$/N−C-800.

characterization techniques were performed including TEM, XRD, N_2 adsorption/desorption isotherms, and XPS. First, the cobalt contents in the Co_x/N−C-800 samples were measured by ICP-AES. As shown in Table S1, the exact Co contents of $Co_{0.01}$/N−C-800, $Co_{0.05}$/N−C-800, and $Co_{0.20}$/N−C-800 were 0.01, 0.05, and 0.20 wt %, respectively. Figure 1 shows N_2 adsorption−desorption isotherms and the corresponding pore size distribution of $Co_{0.05}$/N−C-800. Notably, the samples show typical type-IV isotherms, giving a steep increasing at a relative pressure 0.5 < P/P_0 < 0.95, which is characteristic of the presence of mesoporosity. The $Co_{0.05}$/N−C-800 sample has the largest surface area of 804 m^2/g, while the surface area of $Co_{0.01}$/N−C-800 and $Co_{0.20}$/N−C-800 is 754 and 586 m^2/g, respectively. The significant reduction in the surface area in $Co_{0.20}$/N−C-800 is due to an excess introduction of a large amount of Co metal in the sample.
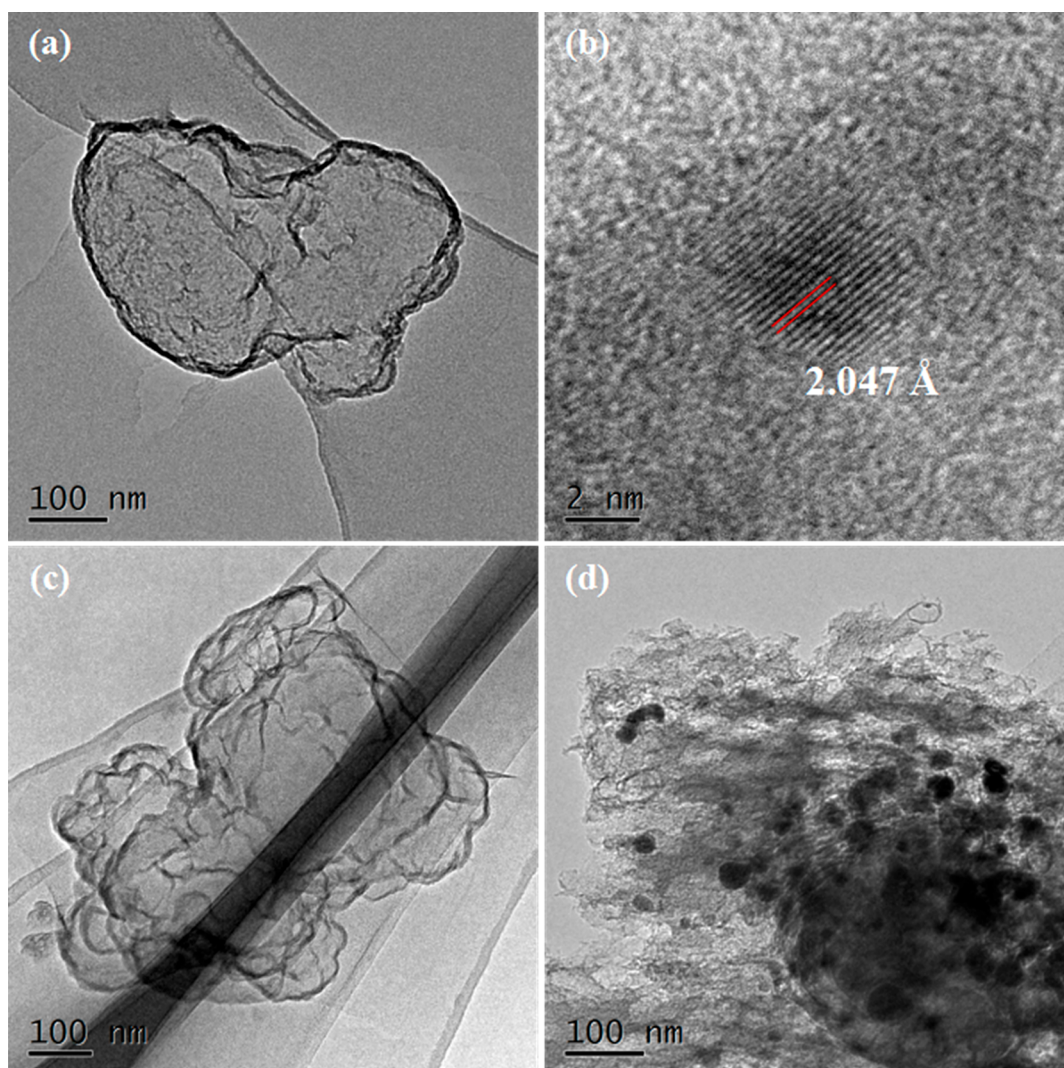
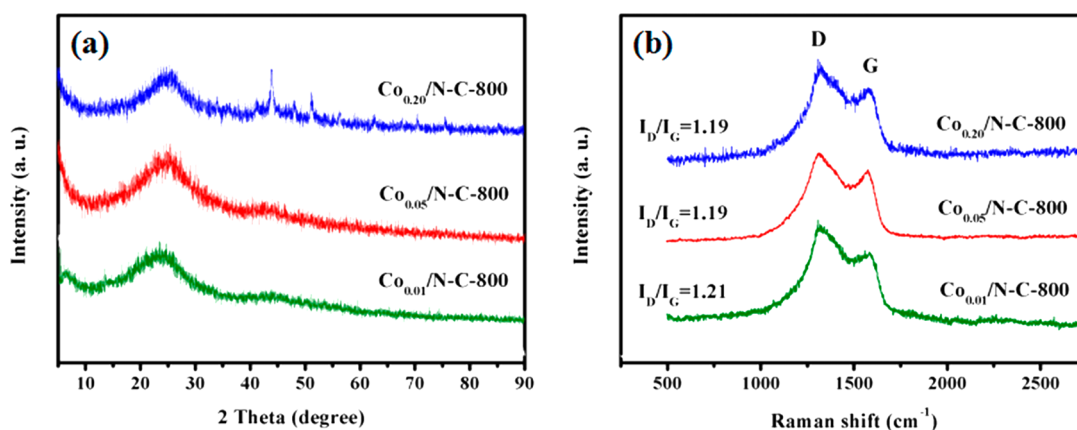**Figure 2.** (a, b) TEM and HRTEM images of $Co_{0.05}/N-C-800$, (c) TEM image of $Co_{0.01}/N-C-800$, and (d) TEM image of $Co_{0.20}/N-C-800$.

Figure 3. (a) XRD pattern and (b) Raman spectra of $Co_x/N-C-800$ samples.

Moreover, the mesoporous $Co_{0.05}/N-C-800$ sample shows a pore-size distribution at 4.0 nm (Figure 1b).

The morphology of the as-prepared $Co_x/N-C-800$ catalysts was characterized by TEM and HRTEM (Figure 2). Figure 2a shows a sheetlike nanostructure, indicating that the ZIF-8 framework collapsed and graphitized under high annealing temperature. It is also seen from Figure 2b that the crystallized Co nanoparticles were highly dispersed as tiny clusters with a size of about 4 nm and surrounded by graphitized carbon support. The lattice spacing of the Co was measured to be 2.047 Å, which corresponds to the well-crystallized Co(111) planes (PDF#15-0806).[25,26] Moreover, the structure of $Co_{0.01}/N-C-800$ (Figure 2c) was similar to the morphology of $Co_{0.05}/N-C-800$, but it is very hard to observe Co
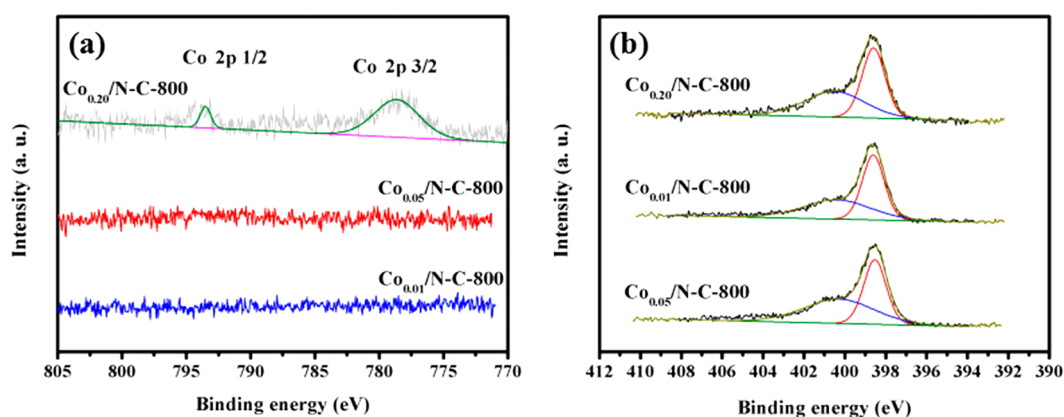
Figure 4. (a) Co 2p spectra and (b) N 1s spectra of $Co_x/N-C-800$ samples.

Table 1. Catalytic Performance of Different Catalyst Samples in Allylic Oxidation of α-pinene under Solvent-Free Conditions[a]

entry	catalyst	conv. of **1a** (%)	yield of **1b** (%)	yield of **1c** (%)	yield of **1d** (%)	yield of **1e** (%)
1	$Co_{0.01}/N-C-800$	57	14	20	18	2
2	$Co_{0.05}/N-C-800$	90	<1	4	85	
3	$Co_{0.20}/N-C-800$	71	5	20	41	3
4	$Co_{0.05}/N-C-950$	89	5	17	62	3
5[b]	$Co_{0.05}/N-C-800$	5	4	1		
6		22	10	7	5	
7[c]	$N-C-800$	45	10	18	17	
8	$Co(acac)_2$	68	21	13	29	
9	$N-C-800/Co(acac)_2$	66	21	23	20	
10[d]	$Co_{0.05}/N-C-800$	10	<1	6	3	1
11[e]	$Co_{0.05}/N-C-800$	19	3	8	8	

[a]Reaction conditions: α-Pinene (1.00 g), catalyst (0.05 g), O_2 balloon, 85 °C, 24 h. Conversion and yield were measured by GC. [b]N_2 balloon. [c]Pyrolyzed from ZIF-8. [d]Phenol (15 mmol, 1.46 g). [e]TEMPO (12 mmol, 1.87 g).

Table 2. Results of the Selective Oxidation of α-Pinene Using $Co_{0.05}/N-C-800$ and Other Reported Catalysts

entry	reaction conditions	conv. of **1a** (%)	sel. of **1d** (%)	TOF (mol verbenone mol^{-1} Co h^{-1})	ref
1	$Co_{0.05}/N-C-800$, O_2, solvent-free, 85 °C, 24 h	90	95	615	this work
2	$Co_{0.01}/N-C-800$, O_2, solvent-free, 85 °C, 24 h	57	18	651	this work
3	$Co_{0.20}/N-C-800$, O_2, solvent-free, 85 °C, 24 h	71	41	74	this work
4	Cr-MIL-101, TBHP, solvent-free, 60 °C, 16 h	26	39		34
5	Co-MOR, TBHP, DMF, 90 °C, 5 h	45	20	10	35
6	VO(IV), H_2O_2, water, 60 °C, 8 h	49	55	5	36
7	C_5MnCl, H_2O_2, CH_3CN, 60 °C, 8 h	56	56	21	12
8	$UO_2^{2+}/MCM-41$, TBHP, CH_3CN, 70 °C, 24 h	77	53	57	37
9	$AuCu/TiO_2$, TBHP, CH_3CN, 70 °C, 24 h	97	48	13	14
10	$Ru@HEA_{16}Cl$, TBHP, 20 °C, 3 h	100	34	408	38
11	V-VSB-5, O_2, CH_3CN, 60 °C, 5 h	18	17	-	39
12	Cr-MCM-41, O_2, solvent-free, 60 °C, 3.5 h	40	26	-	13
13	$Fe(III)/SiO_2$, O_2, CH_3CN, 84 °C, 10 h	73	18	15	40
14	MnO_2, O_2, solvent-free, 75 °C, 10 h	94	87	-	41

nanoparticles because of ultralow Co content (about 0.01 wt %). With the metal amount increased to 0.2 wt %, severe metal agglomeration was observed in the obtained $Co_{0.20}/N-C-800$ sample (Figure 2d), suggesting that an excess of metallic cobalt does not dispersed well on the sacrificial template ZIF-8.

Before pyrolysis of Co@ZIF-8, it is validated from Figure S2 that the precursors ZIF-8 and Co@ZIF-8 composite showed

the typical XRD pattern of the standard ZIF-8 crystal.[27,28] Figure 3 shows XRD and Raman profiles of the $Co_x/N-C-800$ samples after annealing Co@ZIF-8 at 800 °C. It was found in Figure 3a that all the samples showed a large diffraction peak at 25.2°, which is assigned to a typical (002) plane of carbon nanosheets, indicating the formation of graphitic-like structure in the pyrolysis process. It was also indicated that the $Co_{0.20}/$

Table 3. Catalytic Performance of $Co_{0.05}$/N−C-800 in Allylic Oxidation of Cinnamyl Alcohol to Cinnamaldehyde[a]

entry	T (°C)	solvent	conv. (%)	yield (%)	TOF (mol cinnamaldehyde mol^{-1} Co h^{-1})
1	100	toluene	98	98	77
2	100	DMF	74	74	58
3	90	dioxane	59	59	46
4	70	acetonitrile	49	49	39
5[b]	100	toluene	42	42	165
6[c]	100	toluene	78	78	15

[a]Reaction conditions: cinnamyl alcohol (1.0 mmol), $Co_{0.05}$/N−C-800 (0.05 g), solvent (3 mL), O_2 balloon, 30 h. [b]$Co_{0.01}$/N−C-800 (0.05 g). [c]$Co_{0.20}$/N−C-800 (0.05 g).
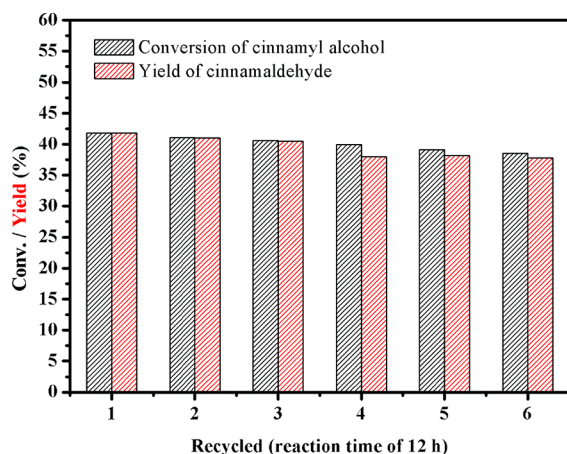
Figure 5. Reusability of the $Co_{0.05}$/N−C-800 catalyst in the selective oxidation of cinnamyl alcohol at 12 h.

N−C with a large metal loading showed characteristic diffraction peaks of metallic cobalt, and the peaks at around 44.1° and 51.5° were assigned to the well-crystallized Co(111) and Co(200), respectively.[29,30] However, the other two samples $Co_{0.01}$/N−C-800 and $Co_{0.05}$/N−C-800 did not display any clear peaks of cobalt species, mainly because the ultralow metal loading was highly dispersed as tiny clusters that are hardly detectable by XRD. This phenomenon is in agreement with a previous report.[31] Moreover, the Raman spectra of three Co_x/N−C-800 samples are shown in Figure 3b. Two peaks are observed at 1317 and 1583 cm^{-1}, which were ascribed to the D and G bands of graphitic carbon planes, respectively. Further, the Co_x/N−C-800 had high intensity ratios of the D to the G band, suggesting that abundant defects were introduced after annealing the precursor ZIF-8.

To gain the valence states of Co and N, the full-range XPS survey shown in Figure S3 confirmed the absence of element Zn in the Co_x/N−C-800 samples because of the vaporization of element Zn at a temperature higher than 700 °C.[24,27] Figure 4 shows the XPS spectra of Co 2p and N 1s for the Co_x/N−C-800 samples. Similar to the XRD characterization results, no peak was found in the Co 2p spectra of $Co_{0.01}$/N−C-800 and $Co_{0.05}$/N−C-800 because of ultralow Co metal loadings and high dispersion. Subsequently, in the cobalt region for $Co_{0.20}$/N−C-800, two major peaks at ca. 793.5 and 778.6 eV assigned to Co 2p1/2 and Co 2p3/2 of metallic Co were observed. The N 1s XPS spectra for the Co_x/N−C-800 materials could be deconvoluted into two peaks with electron binding energies of pyridinic N (398.5 eV) and pyrrollic N (400.3 eV). In addi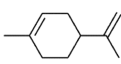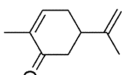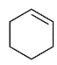tion, the O 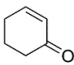1s spectrum was deconvoluted into one peak at 532.0 eV (Figure S4). It can be attributed to the oxygen functional groups such as adsorbed oxygen and a little amount of C−O group on the surface of the sample,[32] showing the absence of cobalt oxide species in Co_x/N−C catalysts.
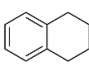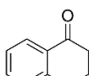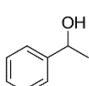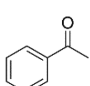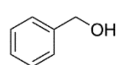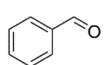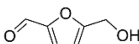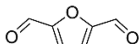
Selective Oxidation of α-Pinene Using $Co_{0.05}$/N−C-800 Catalyst. To study catalytic oxidative performance of the as-prepared Co_x/N−C-y catalysts, we chose α-pinene as the substrate for aerobic allylic oxidation to produce verbenone under solvent-free conditions (Table 1 and Figure S5). Initially, three Co_x/N−C-800 samples with different cobalt loading were tested in this oxidation reaction. It was found 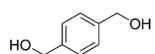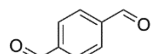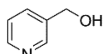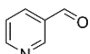that compared with $Co_{0.01}$/N−C-800 and $Co_{0.20}$/N−C-800, $Co_{0.05}$/N−C-800 displayed the highest catalytic activities, with α-pinene conversion of 90% and verbenone yield of 85% (Table 1, entries 1−3). This shows that the metallic cobalt content of Co_x/N−C-800 has a significant effect on their catalytic activities, either too little or too much Co metal content is not good choice for efficient synthesis of verbenone. As shown in Figure 1, $Co_{0.05}$/N−C-800 has indeed the highest BET surface area among all the samples prepared. This implies that $Co_{0.05}$/N−C-800 would have the best exposure of active sites in participating catalytic reaction and thereby leads to excellent catalytic performance. Moreover, the $Co_{0.05}$/N−C-950 catalyst was tested for aerobic oxidation of α-pinene, in which the catalytic selectivity of verbenone was not particularly satisfied (Table 1, entry 4). These results suggest that the annealing temperature is also one key factor affecting the catalytic activity of the $Co_{0.05}$/N−C catalyst. In addition, it was indicated that the oxidation of α-pinene would hardly occur in the absence of catalyst or O_2 (Table 1, entries 5, 6). Also, the N−C-800 sample pyrolyzed from ZIF-8, the precursor Co(acac)$_2$, and N−C-800 with Co(acac)$_2$ induced unsatisfied yields of verbenone (Table 1, entries 7−9).

Furthermore, to clarify the reaction mechanism of allylic oxidation of α-pinene to verbenone, we primarily investigated the reaction pathways of α-pinene oxidation. It was found that verbenol and verbenone were mainly formed in the initial time of 1.5 h, while very little traces of α-pinene oxide and 2,3-pinanediol were detected (Figure S6). With progress of reaction after 2 h, the yield of formed verbenol gradually decreased to 1% at 24 h (Table 1, entry 2), implying that verbenol is a key intermediate at the early stage of this oxidation. These results suggest that α-pinene first undergoes an oxidation reaction over $Co_{0.05}$/N−C-800 to simultaneously form verbenol and verbenone; subsequently, the former compound is further gradually converted into verbenone. In addition, a previous study[33] has demonstrated that both the alcohol verbenol and the ketone verbenone originate from alkoxyl radicals RO·, and the alcohol/ketone ratio would decrease at higher conversion of α-pinene under O_2 atmosphere. The reason for which is because that the reaction of O_2 with RO· radicals is significantly faster and thereby leads to the higher yield of the ketone product. Then we carried out scavenger experiments over the $Co_{0.05}$/N−C-800 catalyst by employing 2,2,6,6-tetramethylpiperidinooxy (TEMPO) and phenol as radicals scavenger. It was seen that the addition of TEMPO and phenol significantly suppressed the selective oxidation of α-pinene, resulting in very low yields for verbenol and verbenone (Table 1, entries 10, 11); this validated that the radicals are the dominant active species accounting for this oxidation reaction.

Comparison of the Performance of $Co_{0.05}$/N−C-800 with Other Catalytic Systems. We have compared the

Table 4. Selective Oxidation of Various Olefins and Alcohols Catalyzed by $Co_{0.05}$/N−C-800[a]

Entry	Substrate	Product	Conv. (%)	Yield (%)
1			85	71
2			73	70
3			61	48
4[b]			70	70
5[b]			99	99
6[b]			94	94
7[c]			99	92
8[b]			86	86

[a]Reaction conditions: Substrate (1.00 g), catalyst (0.05 g), O_2 balloon, 90 °C, 24 h. [b]Substrate (0.10 g), catalyst (0.05 g), toluene (3 mL), O_2 balloon, 100 °C, 30 h. [c]Substrate (0.10 g), catalyst (0.10 g), toluene (3 mL), O_2 balloon, 100 °C, 30 h.

performance and the turnover frequency (TOF) value of $Co_{0.05}$/N−C-800 with other catalysts in the literatures[34−41] for selective oxidation of α-pinene, which is listed in Table 2. It was found that both the conversion of α-pinene and the selectivity of verbenone in most literatures were less than 60%, even though TBHP and H_2O_2 were employed as the terminal oxidant (Table 2, entries 2−5). Several metal composites materials could induce higher conversions, however, the selectivities of verbenone were still below 55% (Table 2, entries 6−8). Moreover, the aerobic oxidation of α-pinene to verbenone using O_2 as the terminal oxidant was also hard to perform with a high selectivity (Table 2, entries 9−12). All in all, most of these results were less than the catalysis performance of $Co_{0.05}$/N−C-800, and the $Co_{0.05}$/N−C-800 catalyst exhibited a high TOF value (615 mol verbenone mol^{-1} Co h^{-1}) for aerobic oxidation of α-pinene to verbenone. This TOF is much higher than those of the state-of-the-art transition-metal-based nanocatalysts reported in the literature. Therefore, compared with the catalyst reported in the literatures, $Co_{0.05}$/N−C-800 can efficiently catalyze aerobic oxidation of α-pinene and achieve high selectivity and excellent yield of verbenone under solvent-free conditions using ambient oxygen molecules as the benign oxidant.

Selective Oxidation of Cinnamyl Alcohol Using $Co_{0.05}$/N−C-800 Catalyst. During the oxidation process of α-pinene using the as-prepared $Co_{0.05}$/N−C-800 catalyst, it is

known that the intermediate verbenol (a kind of allylic alcohol) could be further oxidized to verbenone. In order to obtain the versatility of $Co_{0.05}$/N−C-800 catalyst in selective oxidation of allylic alcohol, the selective oxidation of another allylic alcohol cinnamyl alcohol to cinnamaldehyde was also studied in detailed (Table 3). First, optimization of the reaction condition showed that the highest cinnamaldehyde yield of 98% could be obtained in toluene at 100 °C and 30 h (Figure S7, Table 3, entries 1−4). In comparison to $Co_{0.05}$/N−C-800, $Co_{0.01}$/N−C-800 and $Co_{0.20}$/N−C-800 similarly showed much lower catalytic activities in the oxidation of cinnamyl alcohol (Table 3, entries 5−6). These results again illustrate that the appropriate cobalt content is very important to determine the catalytic activity of Co/N−C-800 catalysts. Moreover, compared with the oxidation of α-pinene, $Co_{0.05}$/N−C-800 displayed a better selectivity (nearly 100%) in aerobic oxidation of cinnamyl alcohol. This shows that $Co_{0.05}$/N−C-800 can be used as an oxidation catalyst for the oxidation of various allylic alcohols using molecular oxygen as an oxidant. The aerobic oxidation of allylic alcohol to α, β-unsaturated aldehydes/ketones has hardly any side reaction over $Co_{0.05}$/N−C-800, whereas the side reaction would occurred in the oxidation of biobased olefins.

Reusability of the $Co_{0.05}$/N−C-800 Catalyst. Figures 5 and S8 shows the reusability of $Co_{0.05}$/N−C-800 in both selective oxidation of α-pinene and cinnamyl alcohol.

Significantly, the catalyst is easily recovered by filtration with very little compromise of catalytic performance. Moreover, a hot filtration experiment for aerobic oxidation of cinnamyl alcohol was conducted and the results are shown in Figure S9. It is expected that no reaction proceeded after the removal of the $Co_{0.05}/N−C-800$ catalyst. This demonstrates that the allylic oxidation of cinnamyl alcohol was intrinsically heterogeneous and the $Co_{0.05}/N−C-800$ catalyst would not leach active species. In addition, N_2 adsorption−desorption, XRD, Raman, and TEM characterization results of reused $Co_{0.05}/N−C-800$ (Figures S10−S13) further confirmed that the catalyst had no obvious change in structure even used for up to six cycles. Thus, the $Co_{0.05}/N−C-800$ catalyst was demonstrated to be highly stable without losing its active sites.

Catalytic Oxidation of Other Olefins and Alcohols. Finally, the applicability of $Co_{0.05}/N−C-800$ was examined for catalyzing aerobic oxidation of different allylic alcohols and biobased olefins. The results are summarized in Table 4. It was found that various allylic alcohols and biobased olefins could be oxidized to corresponding products with relatively good conversions and yields. For example, $Co_{0.05}/N−C-800$-catalyzed aerobic oxidation of cinene afforded carvone with 71% yield (Table 4, entry 1); likewise, cyclohexene, phenylethanol, and 1,2,3,4-tetrahydronaphthalene were oxidized to the target ketones with 48−70% yields (Table 4, entries 2−4). Notably, the selective oxidations of benzyl alcohol and 5-hydroxymethylfurfural to benzyl aldehyde and 2,5-furandicarbaldehyde were observed in up to 99% and 94% yields, respectively (Table 4, entries 5,6). 1,4-Benzenedimethanol and 3-pyridylmethanol gave 92% and 86% yields of 1,4-benzenedialdehyde and 3-pyridinecarboxaldehyde (Table 4, entries 7,8). Taken together, the $Co_{0.05}/N−C-800$ catalyst is readily applicable to synthesize various unsaturated aldehydes or ketones from allylic alcohols and biobased olefins using ambient oxygen molecules as the benign oxidant, thus providing a potentially petroleum-independent solution to those valuable chemicals.

CONCLUSIONS

In summary, this study demonstrates that $Co_{0.05}/N−C-800$ is a highly efficient catalyst with an ultralow Co loading of 0.05 wt % for selective oxidation of α-pinene to verbenone. It can achieve excellent product yield and selectivity under solvent-free conditions using ambient oxygen molecules as the benign oxidant. Moreover, this catalytic system can be also used for selective oxidation of other allylic alcohols and biobased olefins into targeted aldehydes or ketones in good to excellent yields. Several characterization investigations further show that the sacrificial template ZIF-8 plays a key role to disperse well metallic cobalt in the $Co_{0.05}/N−C-800$ catalyst and thus lead to relatively good catalytic performance in such aerobic oxidation. The presented efficient nanocatalyst thus triggers facile synthesis of a series of α,β-unsaturated ketones/aldehydes in high yields.

ASSOCIATED CONTENT

ⓢ Supporting Information

The Supporting Information is available free of charge on the ACS Publications website at DOI: 10.1021/acssuschemeng.8b03678.

GC-MS and GC traces, XRD patterns, XPS spectra, O1s spectra, conversion profiles, reaction profiles, N_2 adsorption-desorption isotherms, Raman spectra, and TEM images (PDF)

AUTHOR INFORMATION

Corresponding Authors
*E-mail: djtao@jxnu.edu.cn (D.J.T.).
*E-mail: licz@dicp.ac.cn (C.Z.L.).
ORCID
Kuan Huang: 0000-0003-1905-3017
Changzhi Li: 0000-0001-6748-2575
Duan-Jian Tao: 0000-0002-8835-0341
Notes
The authors declare no competing financial interest.

REFERENCES

(1) Paradine, S. M.; White, M. C. Iron-catalyzed intramolecular allylic C−H amination. *J. Am. Chem. Soc.* **2012**, *134*, 2036−2039.
(2) Giri, R.; Shi, B. F.; Engle, K. M.; Maugel, N.; Yu, J. Q. Transition metal-catalyzed C−H activation reactions: diastereoselectivity and enantioselectivity. *Chem. Soc. Rev.* **2009**, *38*, 3242−3272.
(3) Brenna, E.; Crotti, M.; Gatti, F. G.; Monti, D.; Parmeggiani, F.; Pugliese, A.; Tentori, F. Biocatalytic synthesis of chiral cyclic γ-oxoesters by sequential C−H hydroxylation, alcohol oxidation and alkene reduction. *Green Chem.* **2017**, *19*, 5122−5130.
(4) Ren, S.; Zhang, J.; Zhang, J.; Wang, H.; Zhang, W.; Liu, Y.; Liu, M. Copper/Selectfluor-System-Catalyzed Dehydration-Oxidation of Tertiary Cycloalcohols: Access to β-Substituted Cyclohex-2-enones, 4-Arylcoumarins, and Biaryls. *Eur. J. Org. Chem.* **2015**, *2015*, 5381−5388.
(5) Shilov, A. E.; Shul'pin, G. B. Activation of C−H bonds by metal complexes. *Chem. Rev.* **1997**, *97*, 2879−2932.
(6) Snider, B. B. Manganese (III)-based oxidative free-radical cyclizations. *Chem. Rev.* **1996**, *96*, 339−364.
(7) Bauer, K.; Garbe, D.; Surburg, H. *Common Fragrance and Flavor Materials*; Wiley-VCH: Weinheim, 1997; p 74.
(8) Meier, M. A.; Metzger, J. O.; Schubert, U. S. Plant oil renewable resources as green alternatives in polymer science. *Chem. Soc. Rev.* **2007**, *36*, 1788−1802.
(9) Neuenschwander, U.; Guignard, F.; Hermans, I. Mechanism of the Aerobic Oxidation of α-Pinene. *ChemSusChem* **2010**, *3*, 75−84.
(10) Wender, P. A.; Mucciaro, T. P. A new and practical approach to the synthesis of taxol and taxol analogs: the pinene path. *J. Am. Chem. Soc.* **1992**, *114*, 5878−5879.
(11) Hu, Q.; Lin, G. S.; Duan, W. G.; Huang, M.; Lei, F. H. Synthesis and Biological Activity of Novel (Z)- and (E)-Verbenone Oxime Esters. *Molecules* **2017**, *22*, 1678−1685.
(12) Mondal, P.; Abdel-Aal, S. K.; Das, D.; Islam, S. M. Catalytic Activity of Crystallographically Characterized Organic-Inorganic Hybrid Containing 1, 5-Di-amino-pentane Tetrachloro Manganate with Perovskite Type Structure. *Catal. Lett.* **2017**, *147*, 2332−2339.
(13) Robles-Dutenhefner, P. A.; Brandão, B. B. N. S.; de Sousa, L. F.; Gusevskaya, E. V. Solvent-free chromium catalyzed aerobic oxidation of biomass-based alkenes as a route to valuable fragrance compounds. *Appl. Catal., A* **2011**, *399*, 172−178.

(14) Ajaikumar, S.; Ahlkvist, J.; Larsson, W.; Shchukarev, A.; Leino, A. R.; Kordas, K.; Mikkola, J. P. Oxidation of α-pinene over gold containing bimetallic nanoparticles supported on reducible TiO_2 by deposition-precipitation method. *Appl. Catal., A* **2011**, *392*, 11−18.

(15) Maksimchuk, N. V.; Timofeeva, M. N.; Melgunov, M. S.; Shmakov, A. N.; Chesalov, Y. A.; Dybtsev, D. N.; Fedin, V. P.; Kholdeeva, O. A. Heterogeneous selective oxidation catalysts based on coordination polymer MIL-101 and transition metal-substituted polyoxometalates. *J. Catal.* **2008**, *257*, 315−323.

(16) Raupp, Y. S.; Yildiz, C.; Kleist, W.; Meier, M. A. R. Aerobic oxidation of α-pinene catalyzed by homogeneous and MOF-based Mn catalysts. *Appl. Catal., A* **2017**, *546*, 1−6.

(17) Han, Y.; Wang, Y. G.; Chen, W.; Xu, R.; Zheng, L.; Zhang, J.; Luo, J.; Shen, R. A.; Zhu, Y.; Cheong, W. C.; Chen, C.; Peng, Q.; Wang, D.; Li, Y. Hollow N-doped carbon spheres with isolated cobalt single atomic sites: superior electrocatalysts for oxygen reduction. *J. Am. Chem. Soc.* **2017**, *139*, 17269−17272.

(18) Han, A.; Chen, W.; Zhang, S.; Zhang, M.; Han, Y.; Zhang, J.; Ji, S.; Zheng, L.; Wang, Y.; Gu, L.; Chen, C.; Peng, Q.; Wang, D.; Li, Y. A polymer encapsulation strategy to synthesize porous nitrogen-doped carbon-nanosphere-supported metal isolated-single-atomic-site catalysts. *Adv. Mater.* **2018**, *30*, 1706508.

(19) Liu, W.; Zhang, L.; Liu, X.; Liu, X.; Yang, X.; Miao, S.; Wang, W.; Wang, A.; Zhang, T. Discriminating catalytically active FeNx species of atomically dispersed Fe-N-C catalyst for selective oxidation of the C−H bond. *J. Am. Chem. Soc.* **2017**, *139*, 10790−10798.

(20) Zhang, Z.; Zhu, Y.; Asakura, H.; Zhang, B.; Zhang, J.; Zhou, M.; Han, Y.; Tanaka, T.; Wang, A.; Zhang, T.; Yan, N. Thermally stable single atom $Pt/m\text{-}Al_2O_3$ for selective hydrogenation and CO oxidation. *Nat. Commun.* **2017**, *8*, 16100−16110.

(21) Yan, H.; Cheng, H.; Yi, H.; Lin, Y.; Yao, T.; Wang, C.; Li, J.; Wei, S.; Lu, J. Single-atom Pd_1/Graphene catalyst achieved by atomic layer deposition: remarkable performance in selective hydrogenation of 1,3-butadiene. *J. Am. Chem. Soc.* **2015**, *137*, 10484−10487.

(22) Zhang, B.; Asakura, H.; Zhang, J.; Zhang, J.; De, S.; Yan, N. Stabilizing a platinum1 single-atom catalyst on supported phospho-molybdic acid without compromising hydrogenation activity. *Angew. Chem., Int. Ed.* **2016**, *55*, 8319−8323.

(23) Qiao, B.; Wang, A.; Yang, X.; Allard, L. F.; Jiang, Z.; Cui, Y.; Liu, J.; Li, J.; Zhang, T. Single-atom catalysis of CO oxidation using Pt_1/FeOx. *Nat. Chem.* **2011**, *3*, 634−642.

(24) Chen, Y.; Ji, S.; Wang, Y.; Dong, J.; Chen, W.; Li, Z.; Shen, R.; Zheng, L.; Zhuang, Z.; Wang, D.; Li, Y. Isolated single iron atoms anchored on N-doped porous carbon as an efficient electrocatalyst for the oxygen reduction reaction. *Angew. Chem.* **2017**, *129*, 7041−7045.

(25) Zhong, W.; Liu, H.; Bai, C.; Liao, S.; Li, Y. Base-free oxidation of alcohols to esters at room temperature and atmospheric conditions using nanoscale Co-based catalysts. *ACS Catal.* **2015**, *5*, 1850−1856.

(26) Li, J.; Liu, G.; Long, X.; Gao, G.; Wu, J.; Li, F. Different active sites in a bifunctional Co@N-doped graphene shells based catalyst for the oxidative dehydrogenation and hydrogenation reactions. *J. Catal.* **2017**, *355*, 53−62.

(27) Zhong, H.; Wang, J.; Zhang, Y.; Xu, W.; Xing, W.; Xu, D.; Zhang, Y.; Zhang, X. ZIF-8 derived graphene-based nitrogen-doped porous carbon sheets as highly efficient and durable oxygen reduction electrocatalysts. *Angew. Chem., Int. Ed.* **2014**, *53*, 14235−14239.

(28) Ye, Y.; Cai, F.; Li, H.; Wu, H.; Wang, G.; Li, Y.; Miao, S.; Xie, S.; Si, R.; Wang, J.; Bao, X. Surface functionalization of ZIF-8 with ammonium ferric citrate toward high exposure of Fe-N active sites for efficient oxygen and carbon dioxide electroreduction. *Nano Energy* **2017**, *38*, 281−289.

(29) Li, J.; Liu, G.; Shi, L.; Xing, Q.; Li, F. Cobalt modified N-doped carbon nanotubes for catalytic C = C bond formation via dehydrogenative coupling of benzyl alcohols and DMSO. *Green Chem.* **2017**, *19*, 5782−6788.

(30) Bai, C.; Li, A.; Yao, X.; Liu, H.; Li, Y. Efficient and selective aerobic oxidation of alcohols catalysed by MOF-derived Co catalysts. *Green Chem.* **2016**, *18*, 1061−1069.

(31) Wang, J.; Huang, Z.; Liu, W.; Chang, C.; Tang, H.; Li, Z.; Chen, W.; Jia, C.; Yao, T.; Wei, S.; Wu, Y.; Li, Y. Design of N-coordinated dual-metal sites: a stable and active Pt-free catalyst for acidic oxygen reduction reaction. *J. Am. Chem. Soc.* **2017**, *139*, 17281−17284.

(32) Long, J.; Xie, X.; Xu, J.; Gu, Q.; Chen, L.; Wang, X. Nitrogen-doped graphene nanosheets as metal-free catalysts for aerobic selective oxidation of benzylic alcohols. *ACS Catal.* **2012**, *2*, 622−631.

(33) Neuenschwander, U.; Guignard, F.; Hermans, I. Mechanism of the aerobic oxidation of α-Pinene. *ChemSusChem* **2010**, *3*, 75−84.

(34) Skobelev, I. Y.; Sorokin, A. B.; Kovalenko, K. A.; Fedin, V. P.; Kholdeeva, O. A. Solvent-free allylic oxidation of alkenes with O_2 mediated by Fe-and Cr-MIL-101. *J. Catal.* **2013**, *298*, 61−69.

(35) Lu, X.-H.; Lei, J.; Wei, X.-L.; Ma, X.-T.; Zhang, T.-J.; Hu, W.; Zhou, D.; Xia, Q.-H. Selectively catalytic epoxidation of α-Pinene with dry air over the composite catalysts of Co-MOR (L) with Schiff-base ligands. *J. Mol. Catal. A: Chem.* **2015**, *400*, 71−80.

(36) lIslam, S. M.; Roy, A. S.; Mondal, P.; Salam, N. Synthesis, catalytic oxidation and oxidative bromination reaction of a reusable polymer anchored oxovanadium(IV) complex. *J. Mol. Catal. A: Chem.* **2012**, *58*, 38−48.

(37) Selvam, P.; Ravat, V. M.; Krishna, V. Selective oxidation of alkenes over uranyl-anchored mesoporous MCM-41 molecular sieves. *J. Phys. Chem. C* **2011**, *115*, 1922−1931.

(38) Rauchdi, M.; Ait Ali, M.; Roucoux, A.; Denicourt-Nowicki, A. Novel access to verbenone via ruthenium nanoparticles-catalyzed oxidation of α-Pinene in neat water. *Appl. Catal., A* **2018**, *550*, 266−273.

(39) Timofeeva, M. N.; Hasan, Z.; Panchenko, V. N.; Prosvirin, I. P.; Jhung, S. H. Vanadium-containing nickel phosphate molecular sieves as catalysts for α-pinene oxidation with molecular oxygen: A study of the effect of vanadium content on activity and selectivity. *J. Mol. Catal. A: Chem.* **2012**, *363*, 328−334.

(40) Mao, J.; Hu, X.; Li, H.; Sun, Y.; Wang, C.; Chen, Z. Iron chloride supported on pyridine-modified mesoporous silica: an efficient and reusable catalyst for the allylic oxidation of olefins with molecular oxygen. *Green Chem.* **2008**, *10*, 827−831.

(41) Pal, P.; Pahari, S. K.; Giri, A. K.; Pal, S.; Bajaj, H. C.; Panda, A. B. Hierarchically order porous lotus shaped nano-structured MnO_2 through $MnCO_3$: chelate mediated growth and shape dependent improved catalytic activity. *J. Mater. Chem. A* **2013**, *1*, 10251−10258.